(This is a sample cover image for this issue. The actual cover is not yet available at this time.)

Remote Sensing of Environment 124 (2012) 174–184

Contents lists available at SciVerse ScienceDirect

Remote Sensing of Environment

journal homepage: www.elsevier.com/locate/rse

Using the Landsat record to detect forest-cover changes during and after the collapse of the Soviet Union in the temperate zone of European Russia

Matthias Baumann [a,*], Mutlu Ozdogan [a], Tobias Kuemmerle [b,c], Kelly J. Wendland [d], Elena Esipova [e], Volker C. Radeloff [a]

[a] Department of Forest and Wildlife Ecology, University of Wisconsin-Madison, 1630 Linden Drive, Madison, WI 53706-1598, USA
[b] Geography Department, Humboldt University Berlin, Unter den Linden 6, 10099 Berlin, Germany
[c] Earth System Analysis, Potsdam Institute for Climate Impact Research (PIK), PO Box 60 12 03, Telegraphenberg A62, D-14412 Potsdam, Germany
[d] College of Natural Resources, University of Idaho, PO Box 441139, Moscow, ID 83844-1139, USA
[e] The Transparent World, Rossolimo str. 5/22, Building 1, Moscow 119021, Russia

ARTICLE INFO

Article history:
Received 18 January 2012
Received in revised form 2 May 2012
Accepted 5 May 2012
Available online xxxx

Keywords:
Forest-cover change
SVM
Temperate forests
Central and Eastern Europe
Post-Soviet land-use change
Logging
Winter imagery
Landsat
Stratified random sample

ABSTRACT

The political breakdown of the Soviet Union in 1991 provides a rare case of drastic changes in social and economic conditions, and as such a great opportunity to investigate the impacts of socioeconomic changes on the rates and patterns of forest harvest and regrowth. Our goal was to characterize forest-cover changes in the temperate zone of European Russia between 1985 and 2010 in 5-year increments using a stratified random sample of 12 Landsat footprints. We used Support Vector Machines and post-classification comparison to monitor forest area, disturbance and reforestation. Where image availability was sub-optimal, we tested whether winter images help to improve classification accuracy. Our approach yielded accurate mono-temporal maps (on average >95% overall accuracy), and change maps (on average 93.5%). The additional use of winter imagery improved classification accuracy by about 2%. Our results suggest that Russia's temperate forests underwent substantial changes during the observed period. Overall, forested areas increased by 4.5%, but the changes in forested area varied over time: a decline in forest area between 1990 and 1995 (−1%) was followed by an increase in overall forest area in recent years (+1.4%, 2005–2010), possibly caused in part by forest regrowth on abandoned farmlands. Disturbances varied greatly among administrative regions, suggesting that differences in socioeconomic conditions strongly influence disturbance rates. While portions of Russia's temperate forests experienced high disturbance rates, overall forest area is expanding. Our use of a stratified random sample of Landsat footprints, and of summer and winter images, allowed us to characterize forest dynamics across a large region over a long time period, emphasizing the value of winter imagery in the free Landsat archives, especially for study areas where data availability is limited.

1. Introduction

Land-cover and land-use-change (LCLUC) is one of the most important components of global environmental change (Foley et al., 2005). Among the different land cover classes, changes in forests are particularly important because of their ability to sequester atmospheric carbon sequestration and their potential to help mitigating climate change (Bonan, 2008; FAO, 2010). Remote sensing has played a key role in monitoring forest change at multiple scales and in different regions of the world (Hansen et al., 2008; Kennedy et al., 2011; Potapov et al., 2011).

LCLUC is often linked to socio-economic changes, leading to conceptual models that describe LCLUC as a function of a country's economic development (e.g., Foley et al., 2005; Lambin et al., 2003). However, these conceptual models usually assume relatively continuous development of political and economic conditions, and it is less clear how drastic and rapid changes in political and economic decisions affect land use. A prime example of a drastic change is the collapse of the Soviet Union in 1991. The switch from a state-controlled economy towards an open market system, and the institutional transformation in Russia resulted in major changes in forest legislation, and the privatization of both the timber industry (Turnock, 1998; Wendland et al., 2011) and the agricultural sector, which had substantial influences on agricultural intensity (Lerman, 2009; Prishchepov et al., in review).

Forest cover changed markedly in many parts of Eastern Europe after the collapse of the Soviet Union, and remote sensing has played a key role in mapping these changes. For example, analyses of Landsat Thematic Mapper (TM) and Enhanced Thematic Mapper Plus (ETM+) data in the Carpathians revealed that the transition period after the breakdown of the Soviet Union was partially characterized by widespread forest harvests (Griffiths et al., 2012; Knorn et al., 2012; Main-Knorn et al., 2009), including illegal logging (Kuemmerle et al., 2009). In European

* Corresponding author. Tel.: +1 608 265 9219; fax: +1 608 262 9922.
E-mail address: mbaumann3@wisc.edu (M. Baumann).

0034-4257/$ – see front matter © 2012 Elsevier Inc. All rights reserved.
doi:10.1016/j.rse.2012.05.001

Russia's boreal forest, harvesting rates were about 1.5% between 2000 and 2005 according to a wall-to-wall analysis of Landsat data (Potapov et al., 2011). In addition to Landsat based studies, European Russia was also part of studies that investigated global forest-cover changes using the Moderate Resolution Imaging Spectroradiometer (MODIS) (Hansen et al., 2010; Potapov et al., 2008). However, past studies either focused on a large area over a short and recent time period, or they analyzed long-term change, but were geographically limited to a smaller study area. What is lacking is a study of the temperate forests of European Russia that analyzes a long time series in the entire region.

One reason that such a study has not been undertaken previously is the quality and volume of data that is needed, in both the spatial and temporal domain. While MODIS imagery provides very frequent information for large areas, these observations are made at moderate spatial resolution (250 to 500 m), which limits their utility for small scale landscape changes. Moreover, since MODIS only started recording the Earth's surface in 2000, the timeframe of available data is too short to analyze forest-cover changes during the last years of socialism and the early post-socialist period. On the other hand, Landsat sensors (especially TM and ETM+) provide high-resolution data (30 m) that are available continuously from 1984 to the present, which makes them ideal for addressing questions of post-Socialist forest-cover change. However, Landsat sensors' relatively narrow swath width (approximately 185 km) makes Landsat data more challenging to use wall-to-wall across large areas. The lower temporal repeat cycle (16 days, 8 days when considering the overlap areas to neighboring footprints in higher latitudes) as one consequence of the narrow swath width and frequent obstructions by clouds lead in some regions of the world to a maximum of 1–2 suitable images per growing season at best, making wall-to-wall-coverage across large areas impossible. An alternative approach for describing forest dynamics across a larger region is to statistically sample a subset of Landsat footprints, greatly reducing the amount of data needed. Such an approach has been used for the United States as part of the North American Forest Dynamics (NAFD) project (Goward et al., 2008) in which 23 footprints were selected and analyzed using Landsat Time Series Stacks (LTSS; Huang et al., 2009a). Similarly, agricultural expansion on expense of intact forests has been investigated in the tropics (Gibbs et al., 2010). Achard et al. (2002) studied the world's humid tropical forests in the TREES-2 project using a sample of overall 100 Landsat scenes (quarters and full scenes). These scenes were selected using a deforestation risk map, which had been created previously based on expert knowledge, and considered higher sampling probabilities in deforestation hot spot areas. The FAO Forest Resources Assessment 1990 used a stratified sample of 117 Landsat TM scenes in the tropics containing at least 10,000 km^2 land surface (FAO, 1996) to assess forest cover. For an analysis of the European Union using a sample of Landsat TM scenes, Gallego (2005) selected his sample based on Thiessen polygons and a stratification process. Stehman (2005) generally showed that focusing on a sample rather than on the entire population yields better estimates, when the improvement of error during the analysis of the sample outweighs the introduction of the sampling error. As such, in the present study, we focused on a sample of Landsat footprints rather than on a wall-to-wall coverage.

Our study also focuses on capturing local and regional forest-cover changes which, we assume, vary across the entire region. Caused by the low data availability that did not allow us to cover the region wall-to-wall for our entire time period of interest, we used a stratified random sample and selected 12 Landsat footprints across the temperate zone of European Russia.

While the use of a statistical sample reduces the number of footprints necessary to study, it does not completely eliminate the problem that cloud-free imagery during the growing season is often limited. Leaf-off imagery in spring and fall can result in classification errors between deciduous trees and non-forested vegetation classes (Reese et al., 2002). We hypothesized that the additional use of a winter image can help overcome this issue, especially for the accurate delineation of forest boundaries. Landsat imagery from the winter season can be useful because of the strong radiance contrast in these areas during the winter (Liira et al., 2006; Peterson et al., 2004). Grasslands and open spaces are completely covered with snow during the winter, leading to high visible reflectance while deciduous and needle leaf forests have a lower reflectance due to branches and shadows. In other words, adding a second image from the winter period of the same year may possibly increase the overall accuracy of the classification by helping to distinguish grass areas from deciduous forests. The use of winter imagery has been successfully shown in the past: their addidional use led to an accuracy of 89% for quantification of bamboo understory growth in a mixed forest area (Wang et al., 2009). Winter imagery use was also reported providing an alternative to hyperspectral data for mapping forest wildlife habitat in the central and southern Appalachians (Tirpak & Giuliano, 2010). In the most recent study, Stueve et al. (2011) tested snow-covered Landsat imagery in North America and found that they reduce commission errors of disturbance areas by nearly 28%. Based on these prior findings, we decided to investigate if winter imagery can also improve forest/non-forest-classifications in the temperate region of Russia.

Another shortcoming of most prior studies in European Russia is that they examined only permanent forests and forest disturbances, while ignoring forest recovery (defined here as forest regeneration on disturbance sites, as well as forest expansion onto land that was not forested at the beginning of the Landsat record). Rates of forest recovery are of paramount importance for studies of carbon sequestration both above ground (Böttcher et al., 2008; Houghton, 2005) and in the soil (Guo & Gifford, 2002). Forest recovery is particularly important in the former Soviet Union and Eastern Europe (Vuichard et al., 2008). For example, widespread farmland abandonment (as documented by Baumann et al., 2011; Kuemmerle et al., 2008; Prishchepov et al., in review) suggests that large areas of former farmland are reverting to forests, which creates a large carbon storage potential (Kuemmerle et al., 2011; Olofsson et al., 2011). However, the extent and the intensity of forest recovery in the temperate zone of European Russia are not well known.

The overarching goal of our study was therefore to characterize regional differences of post-socialist forest-cover changes in the temperate region of European Russia using a representative sample of Landsat footprints. More specifically, our objectives were to:

- quantify the changes in forested areas in 5-year-increments from 1985 to 2010 across a stratified random sample of 12 Landsat footprints,
- determine forest recovery rates in these footprints before and after the collapse of the Soviet Union and compare these patterns with those in other eastern European countries, and
- test whether the inclusion of a winter image increases classification accuracy.

2. Study area

Our study region included three Russian federal districts, 27 federal districts (hereafter: 'regions'), which are subdivided into 821 municipal districts (Fig. 1). The two largest cities of European Russia, St. Petersburg and Moscow, were located in our study region. Russia contains 20% of the world's forests (about 809 million ha; FAO, 2010), and in the temperate region, temperate coniferous, broadleaf, and mixed forests dominate the landscape.

European Russia's forest sector and forest legislation underwent several substantial changes since 1991, including privatization of the timber industry, and changing decentralizations and re-centralizations of the forest administration between federal, local and regional administrators (Eikeland et al., 2004; Wendland et al., 2011). Based on the 1993 *Principles of Forest Legislation*, forest management and

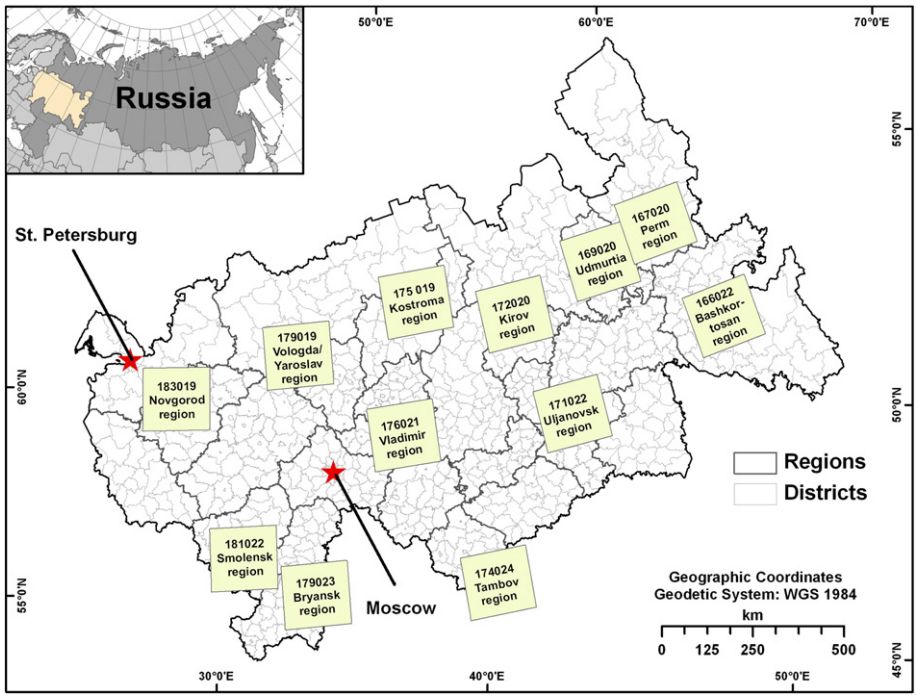

Fig. 1. The temperate zone of European Russia with its administrative deviation, and the Landsat footprints, selected for classification.

administration were decentralized to local forest administrators, giving them responsibility for forest management activities, including sanitary cuts, thinning, and reforestation. Concurrent privatization of logging enterprises and wood processing centers did not stop highly inefficent wood utilization and poor management of forest areas that was present during Soviet times (Krott et al., 2000). In 1997, Russia issued its first forest code, which recentralized the decision making authority first to the regional level, and later to the federal level, and one aim was to stop illegal harvesting activities (Torniainen et al., 2006). In the latest version of the Forest Code, Russia again decentralized decision-making to the regional level, while at the same time designating responsibilities for forest resource use to private timber firms (Torniainen & Saastamoinen, 2007).

Similar to the forest sector, the agricultural sector underwent substantial changes after 1991. The introduction of a market-driven economy resulted in the end of most agricultural subsidies. Together with rural population decline wide areas of agricultural land were abandoned (Lerman, 2009), many of which are now reverting back to forests (Prishchepov et al., in review).

3. Data and methods

3.1. Data and pre-processing

We used a stratified random sample of 12 Landsat footprints that we were confident of being able to represent the variability of forest areas and forest-area changes across the temperate region of European Russia. To select a representative sample we stratified our study area by forest cover, and selected a random sample of footprints from each stratum. We stratified the Landsat footprints by forest cover using the 2005 MODIS vegetation continuous field (VCF; Hansen et al., 2006), to ensure that our sample contained areas of higher and lower proportion of forest cover in the landscape. Our interest was to analyze the differences among administrative regions and these differences affect forest-cover patterns. Thus we calculated the mean value of the mean tree canopy cover for each administrative region, and divided the regions into five forest cover categories of approximately even size. We then attached the Landsat footprints that overlaps each region and randomly selected two footprints from each category and one additional footprint from the two categories with the highest forest cover. With this method, a Landsat footprint always contained the information of the administrative region it overlaps with most (Fig. 1). This way we were able to capture the variability of forest cover within the study region with extra attention given to forested areas. This gave a total sample size of 12 Landsat footprints. For each footprint we selected six images, representing 5-year-intervals from 1985 to 2010. We used data from the Landsat sensors TM4 and TM5 as well as from Landsat ETM+ prior to May 2003. We avoided using ETM+ imagery for the time periods after May 2003 because of the scanline corrector (SLC) data gap issue. We selected images that (a) had no or very low cloud contamination, (b) were recorded during the growing season, and (c) were closest to the year of interest (i.e., 1985, 1990, 1995 etc.). 71 out of 76 images were acquired from the United States Geological Survey (USGS, 2006) in terrain-corrected quality (L1T) and the remaining images were co-registered to these images using automated tie-point collection (Kuemmerle et al., 2006). We included the Space Shuttle Topography Mission (SRTM) digital elevation model (resampled to 30 m) in the co-registration process to account for relief displacement. The average positional error of the co-registered images was less than 0.20 pixel (or less than 6 m). Some images showed contamination by clouds, which were digitized and masked.

3.2. Training and image classification

The task of classifying 72 Landsat scenes (12 footprints with six time steps each) necessitated that we used a training strategy to minimize the overall training effort while maximizing classification accuracy. To do this, we first classified the 2010 image of every footprint using the Iterative Self Organizing Data Analysis Technique (ISODATA) unsupervised classification algorithm into 40 classes and labeled each class either as 'forest' or 'other land cover'. Within both 'forest', and 'other land cover' we randomly sampled 1000 points, ensuring a minimum distance of 2000 m between points to minimize spatial auto-correlation. We then labeled each point as either 'forest' or 'other land cover'. Points were considered 'forest', if they covered at least one Landsat pixel (30×30m) and their tree cover exceeded 60%, corresponding to the category of 'closed tree cover' in the Land

Cover Classification system by Di Gregorio (2005). This means that our forest definition included orchards, but not single trees, rows of tree or open shrublands. Our criteria of 60% canopy cover was also more restrictive than the FAO definition where forest is "land with tree crown cover (or equivalent stocking level) of more than 10% and an area of more than 0.5 hectares (ha)" (FAO, 2010).

To reduce the size of training data, we only considered points that had constant land cover over the entire time period. In other words, rather than labeling training points for each image of a given footprint separately, we analyzed all six images of a footprint simultaneously and considered only points that were consistently characterized as 'forest' or 'other land cover' in all six images (Kuemmerle et al., 2009). We based our decision for each point on the visual interpretation of the Landsat imagery and high resolution Quickbird imagery from Google Earth™. The Quickbird images were only used for confirmation and validation purposes as they were not available for the entire area and their image acquisition varied across our sample. Yet, they also provided useful information when a point was not directly covered by high resolution imagery, because in most cases in the neighborhood of the points high resolution coverage was available and the signature in the Landsat imagery was the same as at the actual point location. This increased the confidence of our labeling decision for each point as it was made based on the best information available. The 'consistency requirement' of our training data dictated that recovering forests be excluded, because no confident decision could be made to determine in every case that the land cover label satisfied our requirement of tree cover exceeding 60%. This strong conservative rule set for each point enabled us to generate one training dataset, which was applicable for each image within a footprint, greatly reducing the time for gathering the training data. At the same time, the pre-stratification using the ISODATA caused that despite these set of rules we had greater than1750 points on average per footprint available for classification and validation.

We used Support Vector Machines (SVM) to classify our images. SVM fit a linear hyperplane between two classes in a multi-dimensional feature space (Foody & Mathur, 2004a) by maximizing the margin between training samples of opposite classes. In the case of two non-linearly separable classes, SVM use kernel functions to transform training data into a higher dimensional feature space where linear separation is possible (Huang et al., 2002). The exclusive focus on pixels at the class boundaries (Foody & Mathur, 2004b, 2006), and the ability to handle non-linear separation boundaries, makes SVM very efficient in handling complex class distributions (Huang et al., 2002; Pal & Mather, 2005).

In the first step we parameterized a SVM-model using our training dataset and selected as a kernel function a Gaussian radial basis function. This function requires setting two parameters, which are training data dependent and hard to estimate a-priori: γ, describing the kernel width, and the regularization parameter C, that controls the trade-off between maximizing the margin and training error (Pal & Mather, 2005). While small C-values tend to ignore outliers, large C-values may lead to overfitted SVM models depending on the variability of the training samples. To find the best γ–C-combination, we tested a wide range of combinations of these parameters and compared all models using cross-validation (Janz et al., 2007; Kuemmerle et al., 2008). We then selected the best performing model and classified each of the 72 Landsat TM/ETM+ images using the six reflective spectral bands and retrieved forest/non-forest maps for each of the six time steps. The changes between these time-steps were finally assessed using post-classification map comparison (Fig. 6; Coppin et al., 2004).

Following image classification, we performed an accuracy assessment in three steps. In the first step, we assessed the accuracies for each classification individually. To do this we split our ground truth points into classification and validation points (90% and 10% of the overall points, respectively). Using the validation sample, we then assessed the accuracy of the classification, calculated the error matrix, and derived overall accuracy, user's and producer's accuracy, and the kappa statistic (Congalton, 1991; Foody, 2002). Additionally we calculated the F-measure that characterizes the overall classification accuracy by calculating weighted mean values of user's and producer's accuracy (van Rijsbergen, 1979). For each image, we parameterized ten SVM using different combinations of training and validation points and averaged the resulting accuracy measures to derive robust accuracy estimates for each classification (Steele, 2005). The final image classification then was carried out using all ground truth points of our sample, rendering the accuracy measures conservative estimates (Burman, 1989). We also corrected our accuracy measures for possible sampling bias (Card, 1982) and calculated confidence intervals around the area estimates (Stehman, 2012).

In the second step we assessed the accuracy for a subset of our change maps. To do this, we randomly selected six out of the 60 change maps. For each of these change maps we converted the raster-map into polygons. As a reference, we created an image stack of the two reference images (e.g., the 1985 and the 1990 image for a 1985–1990 change map) and segmented the stack using a nested hierarchical scene model segmentation approach (Woodcock & Harward, 1992). We then randomly selected 100 polygons of at least 1 ha size (equaling 12 pixels) for each class in the change map and compared it with the segments in the original images. We assigned a validation polygon to the class (constant forest, constant other, forest disturbance, forest recovery) based on visual interpretation of how the majority of the pixels in the polygon developed over time. For each class, we then calculated the same accuracy measures as for the single classifications.

Finally, we compared our classifications for the years 2000 and 2005 with a Landsat classification of the same region, made available by Potapov et al. (2011). This dataset is a wall-to-wall coverage of our study region in 60 m resolution. To compare the two classification results, we sampled for every footprint 100 points into each of our two classes and compared the outcome with the classifications by Potapov et al. to derive a measure of agreement.

Some of our initial forest/non-forest classifications were unsatisfactory, mainly when image acquisition dates were either early (e.g., late April/early May) or late (mid to end of October) in the growing season. Detailed analyses of these classifications suggested that most of the classification errors were caused by the confusion between deciduous forest and grassland. We hypothesized that the addition of a second image from the winter season might increase the classification accuracy. We therefore added a winter-season image to the analysis and reran our classifications. We compared the classification results and accuracies of the single image classification with the 2-image stack results, and used the better classification for our analysis. After classifying each image, we applied a majority filter using a minimum mapping unit of 0.5 ha (approximately 6 pixels in a Landsat classification) to remove the salt-and-pepper effect that is typical in raster-based image classifications, but at the same time not omitting smaller scale disturbances.

3.3. Analysis of forest-cover change

To understand how forest cover changed in the temperate region, we analyzed our forest maps in two ways. First, we summarized areas of 'forest' for each footprint separately at each time step, and calculated changes in forested areas. To account for our uneven sample, which had a higher sampling density in the more forested regions, we weighted the percentages of change by the number of footprints within each stratum to obtain an accurate measure of forest-area change across the study region.

Second, we analyzed forest-cover changes at the district level. We calculated the relative net change (RNC) of forest cover throughout the entire period following Kuemmerle et al. (2009) as:

$$RNC = (FC_{2010}/FC_{1985} - 1) * 100 \quad (1)$$

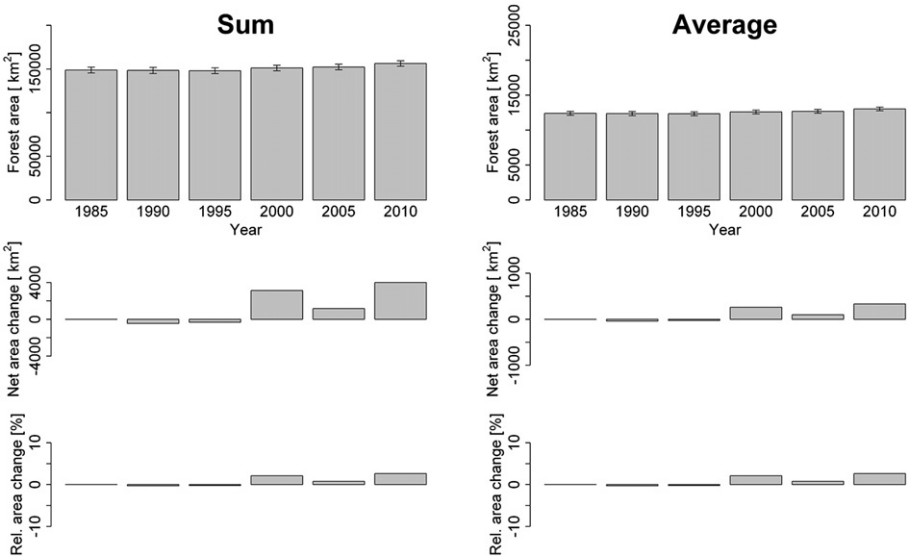

Fig. 2. Area estimates, summarized and averaged across all 12 footprints. The top diagram indicates the overall area at each time step in km^2, including the absolute areas of forest disturbance and forest recovery. The bottom diagram shows the net change of forested areas in km^2 to the previous time-step.

with *FC* as forest cover in km^2 of the described time period. Also at the district level we calculated annual disturbance rates *DR* for each time period as:

$$DR_j = \left(D_j / FCB_j\right) * 100/a \quad (2)$$

where *D* is the overall area of the disturbed forest during the analyzed time period *j*, *FCB* is the forest cover at the beginning of the same time period, and *a* is the number of years between acquisitions, since our acquisition intervals were not equal across footprints (Table 1).

Finally, we calculated proportion of forest area gain per time period FG_j as:

$$FG_j = \left(R_j / NF_{1985}\right) * 100 \quad (3)$$

with R as the area not being forested in 1985 but forested in time period *j* and NF_{1985} is all non-forested area in 1985 (Kuemmerle et al., 2009).

4. Results

Our 72 SVM classifications yielded highly accurate forest/non-forest maps for all footprints across all time periods, with an average accuracy of 95.80% (standard deviation 1.51%, maximum 98.28%, minimum 91.16%) and kappa of 0.96 (0.01, 0.98, 0.91; Table 1). The six selected change maps had an average accuracy of 93.52% (standard deviation 1.32%, maximum 94.47%, minimum 90.96%; Table 2) and a kappa of 0.93 (0.01, 0.94, 0.91). The best classes in the change maps were the persistent classes (forest and other land cover), whereas the change classes had moderately lower accuracies (Table 2). Compared to the classifications by Potapov et al. (2011) we found an agreement of 90% between the two classifications.

Our classifications revealed that in 2010 45.53% of the investigated area was forested (Fig. 2). The amount of forested areas varied across our study region. The regions with the most forest in 2010 were Kostroma (path/row 175/019; 21,541 km^2, 78.4% of the classified area), Novgorod (path/row 183/019; 18,223 km^2, 64.5% of the classified area), and Vladimir (path/row 176/021; 15,863 km^2, 54.3% of the classified area). The regions with the least forest in 2010 were Tambov (path/row 174/024; 2962 km^2, 10.4% of the classified area) and Uljanovsk (path/row 171/022; 6634 km^2, 23.3% of the classified area).

Forest area changed substantially in our study region through the observed period (Fig. 3). Across all 12 footprints, we found a net forest cover increase of 7492 km^2, which corresponds to a weighted increase of 4.5% between 1985 and 2010. The regions with the largest net increase between 1985 and 2010 were Smolensk (551.85 km^2, 9.7%, path/row 181/022) and Kostroma (2257 km^2, 12.3%, path/row 175/019). Other regions only experienced a moderate net forest cover increase, such as Novgorod (647 km^2, 3.6%, path/row 183/019) or Kirov (943.43 km^2, 6.5%, path/row 172/020). In some regions we found a net forest cover decrease between 1985 and 2010, yet the net decreases were smaller than the largest net increases. For example, Uljanowsk (path/row 171/022) and Bashkortostan (path/row 16622) experienced minor decrease in forest area (−215 km^2/−3.1% and −245 km^2/−2.8%). The strongest net forest loss occurred in Tambov (path/row 174/024) with a loss of 455 km^2 (−12.2%).

Changes in forest area also varied across regions during the observed time period. For example, for 6 out of the 12 covered regions (Bashkortostan, Perm, Udmurtia, Uljanowsk, Vladimir, Smolensk) we found a net forest area decrease during the early post-Socialist years (period 1990–1995/2000), but a subsequent net increase in forest area. In some regions the net forest area change was strong enough to exceed Socialist forest area (e.g., Vladimir region with an overall gain of 8.1%). Yet, other regions had less forest now than during Soviet times (e.g., Uljanovsk, net loss of −1.3%). Regions that did not lose forest during 1990–1995/2000 either showed minor increase (e.g., Yaroslav, Tambov or Kirov region) or no significant change in forest area (e.g., Kostroma region). For most of the regions within our stratified random sample, we found a net increase of forest cover either over the last 10 years (strongest increase in the regions Vladimir (11.3%), Bryansk (7.1%), Kirov (6.9%)) or over the last 5 years (strongest increase in the regions Yaroslav (3.8%), Uljanovsk 5.1%, Fig. 3).

Rates of RNC, disturbance and forest recovery varied substantially over time at the regional level (Fig. 4). We found the strongest variation in Bashkortosan (Landsat path/row 166022) during the period 1985–1990 with a standard deviation of 9.42% (max 12.54%, min 2.62%), the lowest within-region variation was 0.10% (0.45%, 0.00%) in Smolensk (path/row 181022). Of all the districts, the highest disturbance rate occurred in a district in Uljanovsk (14.44% period 1985–1990), followed by a district in Kirov (13.11% period 1990–1995), and then Bashkortosan

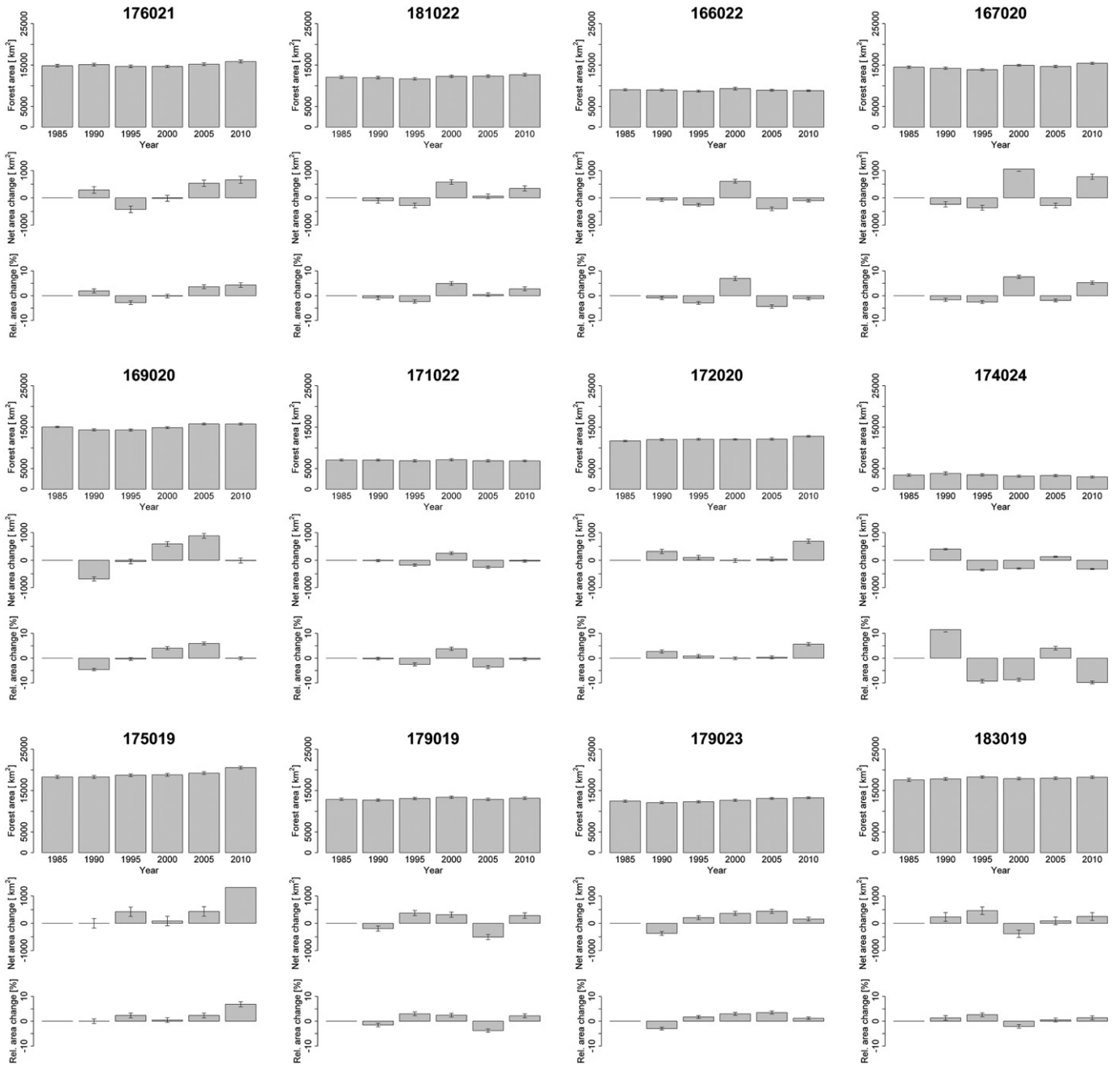

Fig. 3. Forest area estimates for each footprint. The top diagram indicates the overall area at each time step in km^2, including the absolute areas of forest disturbance and forest recovery. The bottom diagram shows the net change of forested areas in km^2 to the previous time-step.

(19.54% period 1985–1990). On the other hand, there were also districts with essentially no disturbance (e.g., in Novgorod 1985–1990, Bryansk 179023, and Uljanovsk 2000–2005). Within-region variation (i.e., different disturbance rates among districts within one region) changed over time in some regions. The highest changes over time occurred in Bashkortosan (standard deviations of 9.42%, 1.26%, 0.80%, 3.94%, 1.73% for the 5 change periods), Vladimir (2.70%, 0.85%, 2.48%, 0.87%, 4.30%), and Kirov (3.04%, 3.20%, 7.07%, 0.92%, 5.26%). The variations within all other regions did not change as strongly over time.

Variations at the district level were also observed for the relative net forest area change. For example, in Bryansk, some districts increased by up to 35.20% in forest area, whereas for other districts decreased by up to −21.31%. In Kostroma all districts gained forest area (max 23.38%, min 1.51%). All other regions contained both districts that gained and districts that lost forest area (Fig. 4).

When acquisition dates were suboptimal, adding a winter image reduced the classification errors in average from 4.38% to 2.50%. On average, the overall classification accuracy (OCA) increased by 1.95% (standard deviation 1.81%), kappa by 0.04 (0.04) and the F-Measure by 1.97% (1.83%; Fig. 5). We found the strongest improvement for 1990 in Landsat footprint 179/023 (increase in overall classification accuracy = 4.08%, Δ kappa = 0.08, Δ F-Measure = 4.13%), and the least improvement in 2000 in footprint 179/023 (increase in overall classification accuracy = 0.22%, Δ kappa = 0.004, Δ F-Measure = 0.23%; Fig. 5).

5. Discussion

Widespread land-use changes have been reported for multiple regions in Eastern Europe for the time period during and after the collapse of the Soviet Union. (Kuemmerle et al., 2011; Wendland et al.,

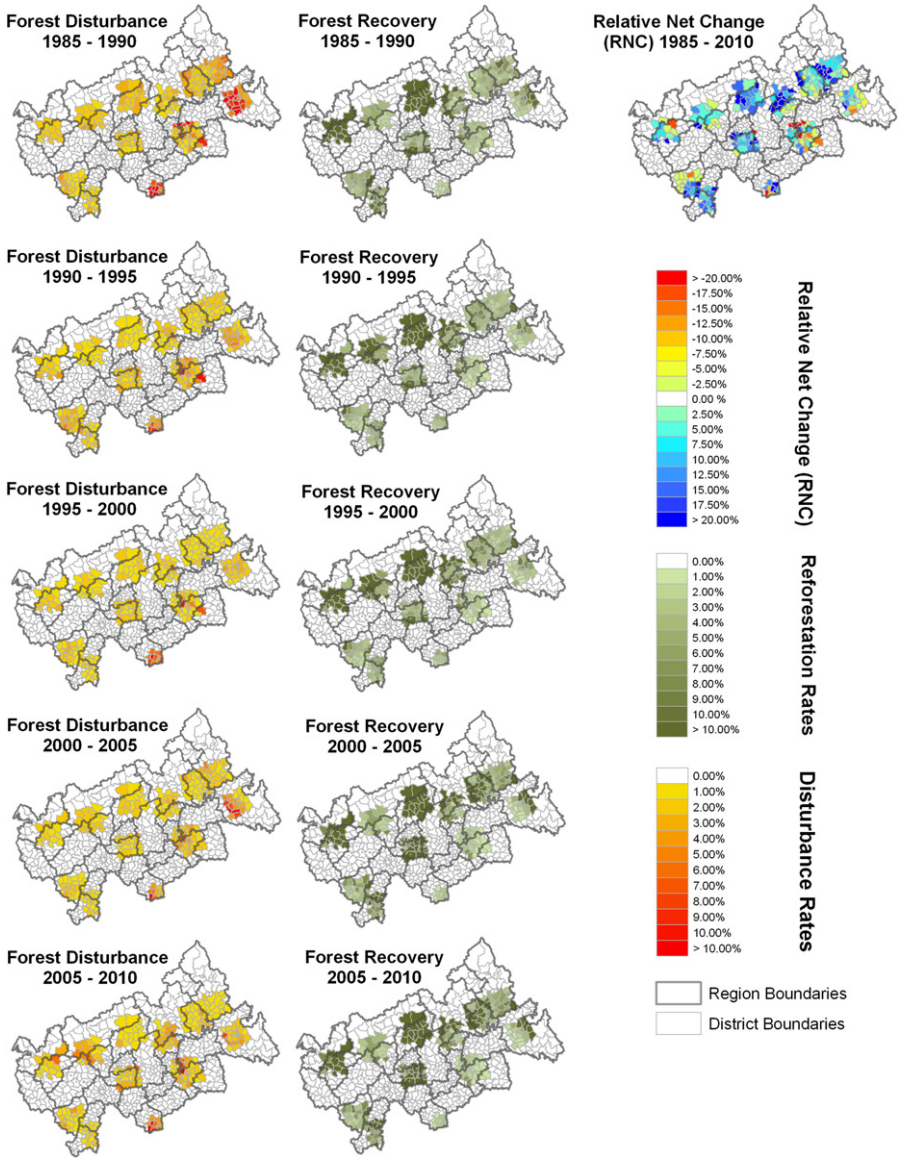

Fig. 4. Rates of forest disturbance and forest recovery per time period (left and middle columns), and relative net change (RNC) of forested area over the entire observation period, aggregated at the district level.

2011). Using a representative subset of 12 Landsat footprints our goal was to analyze regional differences of forest-area changes in the temperate zone of European Russia during and after the collapse of the Soviet Union. The analysis revealed that across our sample forest area initially declined after 1991, but then increased, resulting in a net increase by 2010 of about 6.2% more forest area compared to 1985. However, within our sample, forest-area changes varied substantially over time at both the regional and the district level, sometimes with opposite trends in forest area; suggesting that sub-national differences strongly affect forest cover.

Across samples across the study region, forest cover decreased during the early post-socialist years. This finding matched our expectations,

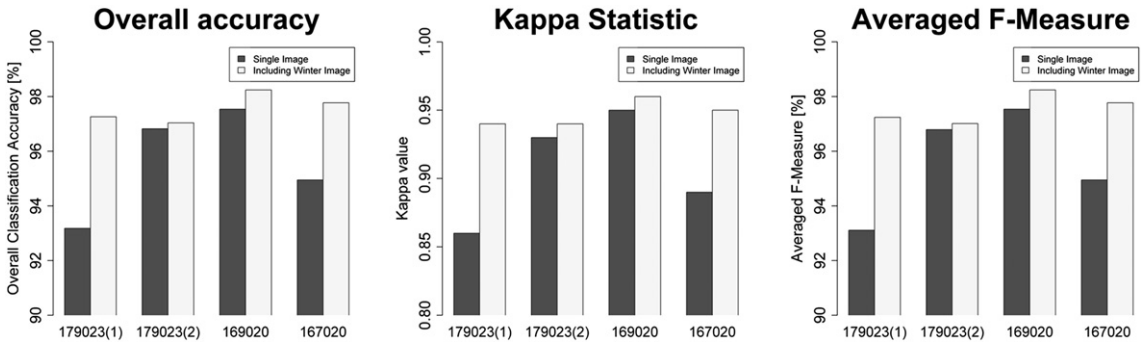

Fig. 5. Difference in classification accuracies after adding a winter-image when image acquisition was sub-optimal.

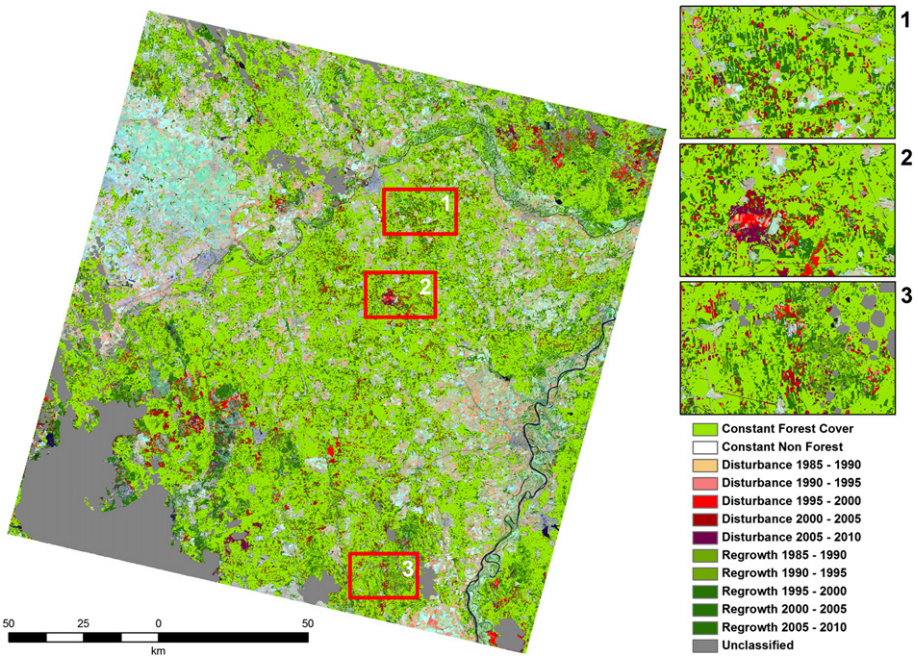

Fig. 6. Forest-cover change map for footprint 176021 (Vladimir region) for 1985–2010.

since other Eastern European studies suggested similar patterns of forest-cover changes after 1991 (Griffiths et al., 2012; Kuemmerle et al. 2007). Surprising, however, was the strong forest-area increase after 2000, and especially after 2005. This forest area increase is most likely a consequence of forest recovery on former disturbed forest areas and a second major land-use change in this region, farmland abandonment. Vast areas of farmland were abandoned after 1991, following the decline in subsidization, rural outmigration, and ownership changes (Lerman, 2009; Mathijs & Swinnen, 1998), and many of these former fields are now covered by shrubs and early successional forests or entirely replaced by planted forests (Prishchepov et al., in review). Furthermore, field visits suggest that even more areas of abandoned farmland may revert to forests in the future, since many abandoned fields exhibit woody vegetation.

The high rates of disturbances and forest recovery in some districts may be overestimations, given that our commission errors for these classes in the change maps are relatively high (Table 3).

We found substantial regional and district differences in forest-cover changes over time at the level of single Landsat footprints. For example, our sample includes regions with little or no changes (e.g., Yaroslav) and regions with substantial changes (e.g., Smolensk) in forest cover between 1985 and 2010 including different spatial-temporal pattern. At the same time we found strong within-region variations (i.e., strong differences at the district level within a region) and very homogenous regions and their forest cover. How can we explain these diverse patterns? Assumingly they are a result of the interaction of several factors that involve changing harvesting practices following changing socio-economic and administrative conditions as well as natural forest disturbance such as fires or windfall. From a socio-economic perspective we see the collapse of the Soviet Union as the main driver which led to decentralization of the forest administration from federal to regional levels following the Principles of Forest Legislation in 1993 and changes in the relative costs and benefits of timber harvesting in these regions (Wendland et al., 2011). The partial autonomy of regions to administer their forests might have led to different strategies of forest management and, possibly, to illegal harvesting at different levels in some regions (Torniainen & Saastamoinen, 2007). The change in relative costs and benefits of timber harvesting would have influenced where timber harvesting occurred following privatization of the timber industry and changes in the overall economic conditions in Russia. As the other main driver for our forest pattern we emphasize the importance of natural disturbances, such as windfall and fires. Our results suggest different rates and patterns of change compared to official statistics. These statistics report, for example, a drop in harvesting rates between 1988 and 1993. For this divergence we see the different types of assessments being the main reason. More specifically, while in our study we mapped forest cover using remote sensing, assessed change rates using post-classification comparison and summarized them under 'disturbance rates', the official statistics exclusively recorded forest harvests on administrative levels and calculated 'harvesting rates'. In other words, our study included all types of disturbance, whereas the harvesting statistics contain harvests only. Given that fires can cause large declines in forest areas, are usually highly variable in time and space, and are present in Russian forests, this could potentially have caused the differences in the rates and patterns of our study compared to rates of official statistics.

Methodologically, our approach showed that analyzing a stratified random sample of Landsat footprints across a large study region is powerful in highlighting regional differences of forest-cover changes Our stratification based on the MODIS VCF product enabled us to capture the entire range of variability of forest cover which revealed being important for highlighting the regional differences. Our approach is thus particularly well suited to situations, where the main goal is to analyze and highlight spatial-temporal variability of forest area across a larger study area when at the same time data availability does not allow for complete coverage.

Similarly, our approach of post-classification map comparison of six binary forest/non-forest maps yielded accurate change maps. Our approach of gathering training data that did not change over time reduced the amount of overall training data for the classification, and hence the time needed to gather these data. This made it possible to perform a long-term analysis with multiple time steps as a series of bi-temporal post-classification comparisons. Hence, our approach may be viewed as a good compromise between traditional bi-temporal change detection methods (Coppin et al., 2004) and more recent trajectory based land-cover change approaches (Kennedy et al., 2011) which require more frequent data than what may be available in many places (Prishchepov et al., in review).

The use of winter imagery increased classification accuracy when available image dates were sub-optimal. Stueve et al. (2011) tested winter imagery and found that their use decreased commission errors,

Table 1
Classified footprints and average classification accuracies. All values represent percentages, except for the kappa-values, which range between 0 and 1, and were obtained by 10-fold cross-validation.

		Overall accuracy	Kappa	User's accuracy		Producer's accuracy		F1-Measure	
				F	NF	F	NF	F	NF
Average accuracies by path/row	176021	94.37	0.95	94.46	93.96	95.32	95.72	92.90	94.83
	181022	95.10	0.951	94.92	95.03	95.16	92.98	96.58	93.99
	171022	97.16	0.972	95.99	96.91	97.24	90.95	99.10	93.82
	179023	97.14	0.97	97.02	97.30	97.07	95.68	98.07	96.48
	169020	96.98	0.97	96.97	97.18	96.81	96.97	96.96	0.971
	167020	96.25	0.96	96.24	96.27	96.26	96.18	96.27	96.22
	175019	93.93	0.94	91.92	93.27	96.11	98.73	81.06	95.92
	174024	95.69	0.96	88.14	95.25	95.73	67.26	99.56	78.67
	166022	96.40	0.96	95.83	95.68	96.73	92.97	98.02	94.30
	179019	95.30	0.95	95.29	94.44	96.14	95.88	94.74	95.15
	172020	97.27	0.97	97.27	96.64	97.90	97.76	96.80	97.19
	183019	94.04	0.94	93.47	93.69	94.73	97.16	88.60	95.39
Average accuracies by time-step	1985	95.59	0.96	94.71	95.55	96.03	93.19	94.66	94.14
	1990	95.38	0.95	94.05	94.98	95.73	91.52	95.04	92.78
	1995	95.93	0.96	94.91	95.86	96.18	92.69	95.55	94.02
	2000	95.89	0.96	94.91	95.32	96.50	93.26	95.05	94.12
	2005	95.89	0.96	94.99	95.65	96.30	93.61	94.90	94.44
	2010	96.13	0.96	95.20	95.44	96.85	94.85	94.13	95.02
Accuracies across all classifications	Mean	95.80	0.96	94.79	95.47	96.27	93.19	94.89	94.09
	STD.	1.51	0.01	2.85	1.76	1.35	8.56	5.23	5.21
	Max	98.28	0.98	98.23	98.18	98.76	99.30	99.75	98.30
	Min	91.16	0.91	81.01	90.68	92.08	51.78	76.56	66.01

leading overall to more accurate classifications. Our results confirmed this. In all cases classification accuracies improved, and in some cases quite substantially so. Despite our already high classification accuracies, we were able to reduce the classification error by over 50% in relative terms. However, our tests were limited to three footprints and only to lower elevation areas (path/row 169/020: mean elevation of 167 m, range between 65 m and 332 m; 179/023: 200 m, 118–287 m; 167/020: 188 m, 60–461 m). We therefore recommend that more detailed studies be conducted in other forest types. Nevertheless, our results are promising, considering that the Landsat archives contain large amounts of winter imagery that have rarely been used for forest classifications in the past.

Our classification results are in strong agreement with the maps developed by Potapov et al. The small difference in agreement is likely a result of the different resolutions of the two data products (30 m in our classification vs. 60 m from Potapov et al.) as well the strategy of generating the training data (manually in our case, completely automated by Potapov et al.)

Despite the high single-map accuracies and the improvement using winter images, some classification errors remained. First, the application of our majority filter may have omitted smaller disturbances and re-growth. Yet, we were able to remove salt-and-pepper noise that is common in raster-based classification approaches. We therefore suggest that the application of such a filter likely improved the classification maps more than introducing errors by omitting small-scale disturbances. As we were mainly interested in investigating large-scale forest-cover trends, this form of omissions of small disturbance patches likely only have a very minor effect on the overall results. Second, positional uncertainties in the Landsat images prevented us from labeling points at the forest/non-forest boundaries, which were subsequently excluded from our analysis. These points were also not included in the accuracy assessment, so that classification accuracies in regions where mixed pixels were widespread are possibly overestimated. Third, the positional uncertainties also possibly influenced the quality of the change classes: our training strategy only considered stable 'forest' and 'non-forest' pixels while not explicitly training on the dynamic classes. This possibly introduced classification errors especially in regions of forest recovery, either after forest disturbance or in case of re-growing forests on abandoned agricultural fields. For example, depending on the spectral characteristics of the landscape manifested in the image, young deciduous forest stands on former agricultural fields, may have been assigned to the 'non-forest' category because their reflective spectra were more similar to an agricultural field during the summer than the forest category. In some cases, this might have lead to omissions of forest recovery in certain time steps, but highlighting them in the following time step. In other words, our training design that focused on the constant classes might have caused that the detected forest

Table 2
Accuracy measures for six randomly selected change-maps. Presented are overall accuracy, kappa for the entire change map; for the classes F (persistent forest), NF (persistent non-forest), D (disturbance) and R (regrowth) user's and producer's accuracy are provided. All values represent percentages, except the kappa values, which range between 0 and 1.

Map	Overall accuracy	Kappa	User's accuracy				Producer's accuracy			
			F	NF	D	R	F	NF	D	R
175019 1985–1990	93.49	0.93	95.00	94.00	78.00	80.00	97.95	88.19	69.32	76.15
179023 1985–1990	94.47	0.85	93.00	97.00	80.00	81.00	98.41	94.51	64.77	68.49
176021 1985–1990	94.20	0.94	96.00	93.00	90.00	80.00	98.76	95.59	44.01	49.85
169020 1990–1995	94.45	0.94	94.00	96.00	88.00	77.00	98.28	94.29	100.0	46.66
181022 2000–2005	90.96	0.91	92.00	91.00	80.00	81.00	96.23	96.20	74.20	24.03
183019 2005–2010	93.52	0.94	94.00	97.00	80.00	78.00	98.57	85.50	80.16	100.0

recovery be assigned to the 'wrong' time step, slightly influencing the spatial-temporal pattern. For the study period and the subset of Landsat footprints (1985–2010) as a whole, however, we are confident of the mapped total area estimates. Finally, the comparison of mono-temporal maps in a time series might have led to an accumulation of classification errors over time. Indeed, the accuracy assessments for our change maps showed accuracy rates that were slightly lower than the theoretical suggestions by Coppin et al. (2004). The validation and the interpretation of accuracy assessments of long classification time series is a problem that has rarely been tackled in the remote sensing literature. Cohen et al. (2011) recently provided a method and tools for the validation and interpretation of dense time stacks. However his framework mainly focuses on time series of annual observations. For many regions of the world, such as the present case, data availability does not allow for annual observations, subsequently leading to other interpretations of detected change. How to handle classification errors that propagate through the time series and how to interpret change products from such analyses, however, has not been investigated yet, despite the fact that this type of analysis will likely gain importance in the future. We therefore suggest that further studies should focus on accuracy measures for long time series that do not consist of annual observations.

6. Conclusions

In this paper we characterized forest-cover changes between 1985 and 2010 in 5-year-intervals for Russia's temperate forests using a stratified random sample of Landsat footprints. Our results suggest that forest cover decreased after 1991, but since 2000, the region experienced a net forest-cover increase especially so after 2005.

The large variations at the regional and district levels and over time indicate that socioeconomic conditions and the major socioeconomic changes, including changes in forest administration and legislation, that occurred after the collapse of the Soviet Union likely influenced forest cover in the temperate region of European Russia.

The regrowth of forests on abandoned farmlands possibly provide important opportunities for carbon sequestration as suggested from studies in other Eastern European regions (Kuemmerle et al., 2011). The detected widespread farmland abandonment in European Russia and the ongoing and observed onset of forest regrowth on these areas could indicate that the region potentially could turn into a large carbon sink in the future.

From a remote sensing perspective, our study makes two main contributions. First, when available data in space and time are limited, sampling a representative subset of Landsat scenes offers the opportunity to study forest-cover changes across a large area over a long time period and to highlight strong spatial-temporal variations of forest-cover change. Second, our study shows for the temperate zone that winter images can be useful to improve classification accuracy when acquisition dates are sub-optimal; and we emphasize the value of winter imagery in forest-cover classifications, given that in some regions of the world data availability is very low.

Acknowledgments

We gratefully acknowledge the support by the Land-Cover and Land-Use Change (LCLUC) Program of the National Aeronautic Space Administration (NASA) through grant NNX08AK77G, the Alexander von Humboldt Foundation, the European Union (VOLANTE FP7-ENV-2010-265104), and the Einstein Foundation. C. Huang provided valuable comments on an earlier version of this manuscript. Dmitry Aksenov and Alexander Prishchepov are aknowledged for helpful discussions. We also would like to thank two anonymous reviewers for useful suggestions to improve this manuscript.

References

Achard, F., Eva, H. D., Stibig, H. J., Mayaux, P., Gallego, J., Richards, T., et al. (2002). Determination of deforestation rates of the world's humid tropical forests. *Science*, *297*, 999–1002.

Baumann, M., Kuemmerle, T., Elbakidze, M., Ozdogan, M., Radeloff, V. C., Keuler, N. S., et al. (2011). Patterns and drivers of post-socialist farmland abandonment in Western Ukraine. *Land Use Policy*, *28*, 552–562.

Bonan, G. B. (2008). Forests and climate change: Forcings, feedbacks, and the climate benefits of forests. *Science*, *320*, 1444–1449.

Böttcher, H., Kurz, W. A., & Freibauer, A. (2008). Accounting of forest carbon sinks and sources under a future climate protocol—Factoring out past disturbance and management effects on age-class structure. *Environmental Science and Policy*, *11*, 669–686.

Burman, P. (1989). A Comparative-study of ordinary cross-validation, v-fold cross-validation and the repeated learning-testing methods. *Biometrika*, *76*, 503–514.

Card, D. H. (1982). Using known map category marginal frequencies to improve estimates of thematic map accuracy. *Photogrammetric Engineering and Remote Sensing*, *48*, 431–439.

Cohen, W. B., Yang, Z., & Kennedy, R. (2011). Detecting trends in forest disturbance and recovery using yearly Landsat time series: 2. TimeSync - Tools for calibration and validation. *Remote Sensing of Environment*, *114*, 2911–2924.

Congalton, R. G. (1991). A review of assessing the accuracy of classifications of remotely sensed data. *Remote Sensing of Environment*, *37*, 35–46.

Coppin, P., Jonckheere, I., Nackaerts, K., Muys, B., & Lambin, E. (2004). Digital change detection methods in ecosystem monitoring: A review. *International Journal of Remote Sensing*, *25*, 1565–1596.

Di Gregorio, A. (2005). *Land Cover Classification System Classification (LCCS)*. Concepts and user manual software version 2. Rome: Food and Agriculture Organisation of the United Nations.

Eikeland, S., Eythorsson, E., & Ivanova, L. (2004). From management to mediation: Local forestry management and the forestry crisis in post-socialist Russia. *Environmental Management*, *33*, 285–293.

FAO (1996). Forest Resources Assessment 1990. *Survey of tropical forest cover and study of change. FAO Forestry Paper, 130*.

FAO (2010). Global forest resource assessment 2010. In Food and Agriculture Organization of the United Nations (Ed.), .

Foley, J. A., DeFries, R., Asner, G. P., Barford, C., Bonan, G., Carpenter, S. R., et al. (2005). Global consequences of land use. *Science*, *309*, 570–574.

Foody, G. M. (2002). Status of land cover classification accuracy assessment. *Remote Sensing of Environment*, *80*, 185–201.

Foody, G. M., & Mathur, A. (2004a). A relative evaluation of multiclass image classification by support vector machines. *IEEE Transactions on Geoscience and Remote Sensing*, *42*, 1335–1343.

Foody, G. M., & Mathur, A. (2004b). Toward intelligent training of supervised image classifications: Directing training data acquisition for SVM classification. *Remote Sensing of Environment*, *93*, 107–117.

Foody, G. M., & Mathur, A. (2006). The use of small training sets containing mixed pixels for accurate hard image classification: Training on mixed spectral responses for classification by a SVM. *Remote Sensing of Environment*, *103*, 179–189.

Gallego, F. J. (2005). Stratified sampling of satellite images with a systematic grid of points. *ISPRS Journal of Photogrammetry and Remote Sensing*, *59*, 369–376.

Gibbs, H. K., Ruesch, A. S., Achard, F., Clayton, M. K., Holmgren, P., Ramankutty, N., et al. (2010). Tropical forests were the primary sources of new agricultural land in the 1980s and 1990s. *Proceedings of the National Academy of Sciences*, *107*, 16732–16737.

Goward, S. N., Masek, J. G., Cohen, W. B., Moisen, G. G., Collatz, G. J., Healey, S., et al. (2008). Forest disturbance and North American carbon flux. *Earth Observing System Transactions*, *89*, 105–116.

Griffiths, P., Kuemmerle, T., Kennedy, R. E., Abrudan, I. V., Knorn, J., & Hostert, P. (2012). Using annual time-series of Landsat images to assess the effects of forest restitution in post-socialist Romania. *Remote Sensing of Environment*, *118*, 199–214.

Guo, L. B., & Gifford, R. M. (2002). Soil carbon stocks and land use change: A meta analysis. *Global Change Biology*, *8*, 345–360.

Hansen, M., DeFries, R., Townshend, J. R., Carroll, M., Dimiceli, C., & Sohlberg, R. (2006). *Vegetation continuous fields MOD44B, 2001 percent tree cover, collection 4.* College Park, Maryland: University of Maryland 2001.

Hansen, M. C., Stehman, S. V., & Potapov, P. V. (2010). Quantification of global gross forest cover loss. *Proceedings of the National Academy of Sciences*, *107*, 8650–8655.

Hansen, M. C., Stehman, S. V., Potapov, P. V., Loveland, T. R., Townshend, J. R. G., DeFries, R. S., et al. (2008). Humid tropical forest clearing from 2000 to 2005 quantified by using multitemporal and multiresolution remotely sensed data. *Proceedings of the National Academy of Sciences of the United States of America*, *105*, 9439–9444.

Houghton, R. A. (2005). Aboveground forest biomass and the global carbon balance. *Global Change Biology*, *11*, 945–958.

Huang, C., Davis, L. S., & Townshend, J. R. G. (2002). An assessment of support vector machines for land cover classification. *International Journal of Remote Sensing*, *23*, 725–749.

Huang, C., Goward, S. N., Masek, J. G., Gao, F., Vermote, E. F., Thomas, N., et al. (2009a). Development of time series stacks of Landsat images for reconstructing forest disturbance history. *International Journal of Digital Earth*, *2*, 195–218.

Janz, A., van der Linden, S., Waske, B., & Hostert, P. (2007). imageSVM—A user-orientated tool for advanced classification of hyperspectral data using Support Vector Machines. *Proceedings of the 5th EARSeL workshop on Imaging Spectroscopy, Bruges, Belgium*.

Kennedy, R. E., Yang, Z., & Cohen, W. B. (2011). Detecting trends in forest disturbance and recovery using yearly Landsat time series: 1. LandTrendr—Temporal segmentation algorithms. *Remote Sensing of Environment*, *114*, 2897–2910.

Knorn, J., Kuemmerle, T., Radeloff, V. C., Szabo, A., Mindrescu, M., Keeton, W. S., et al. (2012). Forest restitution and protected area effectiveness in post-socialist Romania. *Biological Conservation*, *146*, 204–212.

Krott, M., Tikkanen, I., Petrov, A., Tunystsya, Y., Zheliba, B., Sasse, V., et al. (2000). Policies for sustainable forestry in Belarus, Russia and Ukraine. *European Forest Institute Research Report No. 9*. Leiden: Koninklijke Brill NV.

Kuemmerle, T., Chaskovskyy, O., Knorn, J., Radeloff, V. C., Kruhlov, I., Keeton, W. S., et al. (2009). Forest cover change and illegal logging in the Ukrainian Carpathians in the transition period from 1988 to 2007. *Remote Sensing of Environment*, *113*, 1194–1207.

Kuemmerle, T., Hostert, P., Radeloff, V. C., Perzanowski, K., & Kruhlov, I. (2007). Post-socialist forest disturbance in the Carpathian border region of Poland, Slovakia, and Ukraine. *Ecological Applications*, *17*, 1279–1295.

Kuemmerle, T., Hostert, P., Radeloff, V. C., van der Linden, S., Perzanowski, K., & Kruhlov, I. (2008). Cross-border comparison of post-socialist farmland abandonment in the Carpathians. *Ecosystems*, *11*, 614–628.

Kuemmerle, T., Olofsson, P., Chaskovskyy, O., Baumann, M., Ostapowicz, K., Woodcock, C. E., et al. (2011). Post-Soviet farmland abandonment, forest recovery, and carbon sequestration in western Ukraine. *Global Change Biology*, *17*, 1335–1349.

Kuemmerle, T., Radeloff, V. C., Perzanowski, K., & Hostert, P. (2006). Cross-border comparison of land cover and landscape pattern in Eastern Europe using a hybrid classification technique. *Remote Sensing of Environment*, *103*, 449–464.

Lambin, E. F., Geist, H. J., & Lepers, E. (2003). Dynamics of land-use and land-cover change in tropical regions. *Annual Review of Environment and Resources*, *28*, 205–241.

Lerman, Z. (2009). Land reform, farm structure, and agricultural performance in CIS countries. *China Economic Review*, *20*, 316–326.

Liira, J., Pussa, K., & Peterson, U. (2006). The radiance contrast of forest-to-clearcut edges on a medium resolution Landsat Enhanced Thematic Mapper satellite winter image. *International Journal of Remote Sensing*, *27*, 2753–2766.

Main-Knorn, M., Hostert, P., Kozak, J., & Kuemmerle, T. (2009). How pollution legacies and land use histories shape post-communist forest cover trends in the Western Carpathians. *Forest Ecology and Management*, *258*, 60–70.

Mathijs, E., & Swinnen, J. F. M. (1998). The economics of agricultural decollectivization in East Central Europe and the former Soviet Union. *Economic Development and Cultural Change*, *47*, 1–26.

Olofsson, P., Kuemmerle, T., Griffiths, P., Knorn, J., Baccini, A., Gancz, V., et al. (2011). Carbon implications of forest restitution in post-socialist Romania. *Environmental Research Letters*, *6*, 045202.

Pal, M., & Mather, P. M. (2005). Support vector machines for classification in remote sensing. *International Journal of Remote Sensing*, *26*, 1007–1011.

Peterson, U., Pussa, K., & Liira, J. (2004). Issues related to delineation of forest boundaries on Landsat Thematic Mapper winter images. *International Journal of Remote Sensing*, *25*, 5617–5628.

Potapov, P., Turubanova, S., & Hansen, M. C. (2011). Regional-scale boreal forest cover and change mapping using Landsat data composites for European Russia. *Remote Sensing of Environment*, *115*, 548–561.

Potapov, P., Yaroshenko, A., Turubanova, S., Dubinin, M., Laestadius, L., Thies, C., et al. (2008). Mapping the world's intact forest landscapes by remote sensing. *Ecology and Society*, *13*.

Prishchepov, A.V., Radeloff, V.C., Baumann, M., & Kuemmerle, T. Effects of massive socio-economic change on land-use change: Agricultural abandonment during the socio-economic transition in post-Soviet Eastern Europe. *in review*.

Reese, H. M., Lillesand, T. M., Nagel, D. E., Stewart, J. S., Goldmann, R. A., Simmons, T. E., et al. (2002). Statewide land cover derived from multiseasonal Landsat TM data: A retrospective of the WISCLAND project. *Remote Sensing of Environment*, *82*, 224–237.

Steele, B. M. (2005). Maximum posterior probability estimators of map accuracy. *Remote Sensing of Environment*, *99*, 254–270.

Stehman, S. V. (2005). Comparing estimators of gross change derived from complete coverage mapping versus statistical sampling of remotely sensed data. *Remote Sensing of Environment*, *96*, 466–474.

Stehman, S. V. (2012). Impact of sample size allocation when using stratified random sampling to estimate accuracy and area of land-cover change. *Remote Sensing Letters*, *3*, 111–120.

Stueve, K. M., Housman, I. W., Zimmerman, P. L., Nelson, M. D., Webb, J. B., Perry, C. H., et al. (2011). Snow-covered Landsat time series stacks improve automated disturbance mapping accuracy in forested landscapes. *Remote Sensing of Environment*, *115*, 3203–3219.

Tirpak, J. M., & Giuliano, W. M. (2010). Using multitemporal satellite imagery to characterize forest wildlife habitat: The case of ruffed grouse. *Forest Ecology and Management*, *260*, 1539–1547.

Torniainen, T. J., & Saastamoinen, O. J. (2007). Formal and informal institutions and their hierarchy in the regulation of the forest lease in Russia. *Forestry*, *80*, 489–501.

Torniainen, T. J., Saastamoinen, O. J., & Petrov, A. P. (2006). Russian forest policy in the turmoil of the changing balance of power. *Forest Policy and Economics*, *9*, 403–416.

Turnock, D. (1998). Introduction. In D. Turnock (Ed.), *Privatization in rural Eastern Europe. The process of restitution and restructuring* (pp. 1–48). Cheltenham: Edward Elgar.

USGS (2006). *USGS Landsat project [online].*

van Rijsbergen, C. J. (1979). *Information retrieval.* London: Butterworth-Heinemann.

Vuichard, N., Ciais, P., Belelli, L., Smith, P., & Valentini, R. (2008). Carbon sequestration due to the abandonment of agriculture in the former USSR since 1990. *Global Biogeochemical Cycles*, *22*.

Wang, T., Skidmore, A. K., Toxopeus, A. G., & Liu, X. (2009). Understory bamboo discrimination using a winter image. *PE&RS, Photogrammetric Engineering and Remote Sensing*, *75*, 37–47.

Wendland, K. J., Lewis, D. J., Alix-Garcia, J., Ozdogan, M., Baumann, M., & Radeloff, V. C. (2011). Regional- and district-level drivers of timber harvesting in European Russia after the collapse of the Soviet Union. *Global Environmental Change*, *21*, 1290–1300.

Woodcock, C., & Harward, V. J. (1992). Nested hierarchical scene models and image segmentation. *International Journal of Remote Sensing*, *13*, 3167–3187.